# *Supporting Information*

## Dissociating High Concentration Lithium Salts in LLZTO-Based High Dielectric Polymer Electrolytes for Low Temperature Li Metal Batteries

Jiajun Gong, Zhicheng Yao, Qimin Peng, Huizi Tang, Wenhao Han, Shimou Chen*

# 1. Experiments

## 1.1 Material Characterizations

The structure of electrolytes was characterized by Fourier Transform infrared spectrometers (FTIR, Nicolet 6700). The X-ray diffractometer (XRD, Bruker D8 Focus) with a Ni–filtered Cu Kα radiation (λ = 0.15406 nm) source was used to analyze the crystalline state of electrolytes. The field-emission scanning electron microscope (SEM, Zeiss Supra 55VP) with a 5-kV acceleration voltage was carried out to characterize the morphology and structure of anode and electrolytes. X-ray photoelectron spectroscopy (XPS) was obtained by Thermo Scientific K-Alpha instrument. Raman spectroscopy was recorded at room temperature using InVia Reflex with laser excitation at 785 nm. The morphology of the cathode side was analyzed by transmission electron microscopy (TEM, JEOL HEM-ARM200F). Solid-state magic angle spinning $^{7}$Li NMR was performed using a JEOL JNM ECZ600R instrument.

## 1.2 Electrochemical measurements

LFP electrodes and NCM811 electrodes were prepared by mixing 80 wt% of the active substance, 10 wt% of carbon black (Super P), and 10 wt% of PVDF 5130 in a small glass vial containing an appropriate amount of NMP with magnetic stirring for about 8 h. The homogeneous paste was pasted on an aluminum foil with a thickness of 12 μm and dried overnight in a vacuum oven at 80 ℃. The cathodes prepared are loaded at 1.8~2.6mg cm$^{-2}$. When assembling full cells and Li||Li symmetrical cells, the electrode/electrolyte interface is moistened with a commercial low-temperature liquid electrolyte of 5μl to reduce interface impedance. The model of the cells case is C2025. Galvanostatic discharge/charge tests were carried out using the Neware Battery Measurement System. The Autolab electrochemical workstation (manufactured by Metrohm, Switzerland) was utilized to measure Liner sweep voltammetry (LSV), Cyclic voltammetry (CV), and Electrochemical Impedance Spectroscopy (EIS). LSV was conducted at room temperature in a coin cell with symmetrical stainless steel electrodes.

The voltage range tested was 3−6.5 V (V vs $Li/Li^+$), with a scanning speed of 0.1 mV $s^{-1}$. The ionic conductivities of electrolytes were determined with a 2025-type coin sandwiching the membranous between two stainless steel. The electrochemical impedance spectroscopy (EIS) measurements were carried out with 10 mV of AC amplitude over the frequency range from 0.1 Hz to 100000 Hz. The following equation Eq.(1) was used to calculate the ionic conductivity of electrolytes.

$$\sigma = \frac{L}{SR} \quad (1)$$

where σ is the ionic conductivity, L is the distance between two pieces of stainless steel, S is the contact area between the electrolyte and stainless steel, and R is the bulk resistance. The lithium-ion transference numbers ($t_{Li}^+$) of electrolytes were tested on a 2025-type coin sandwiching the electrolyte membranous between two Li by AC impedance and DC polarization. Where the polarization currents (initial ($I_0$) and steady-state ($I_{ss}$)) were measured under a DC polarization voltage of 10 mV (ΔV). The impedances before and after polarization are $R_0$ and $R_{ss}$, respectively. Then the $t_{Li}^+$ was calculated according to the Bruce–Vincent–Evans equation as Eq.(2).

$$t_{Li}^+ = \frac{I_{ss}(\Delta V - I_0 R_0)}{I_0(\Delta V - I_{ss} R_{ss})} \quad (2)$$

The compatibility with Li-anode was shown by the following experiments. The lithium plating−stripping galvanostatic cycling performances of Li|PTCL−1.5|Li symmetric cell under 0.1 mA/$cm^{-2}$. The assembled Li|PTCL−1.5|LFP cells were tested between 2.5 V to 3.8 V for cycling and rate performances after the cells ran for three cycles at a low rate (0.1 C) to ensure the gradual formation of stable SEI layers. Li|PTCL−1.5|NCM9055, Li|PTCL−1.5|NCM811, and Li|PTCL−1.5|$LiCoO_2$ cells were tested at 2.8−4.3 V, 2.8−4.3 V, and 3−4.35 V, respectively. All cells were activated at a low rate (0.1C) for three cycles before further cycling tests. The light plate by the pouch cell experiment has an operating voltage of 1.5 V, a pixel array of 11×44 dots, and dimensions of 93 mm×30 mm×6 mm.

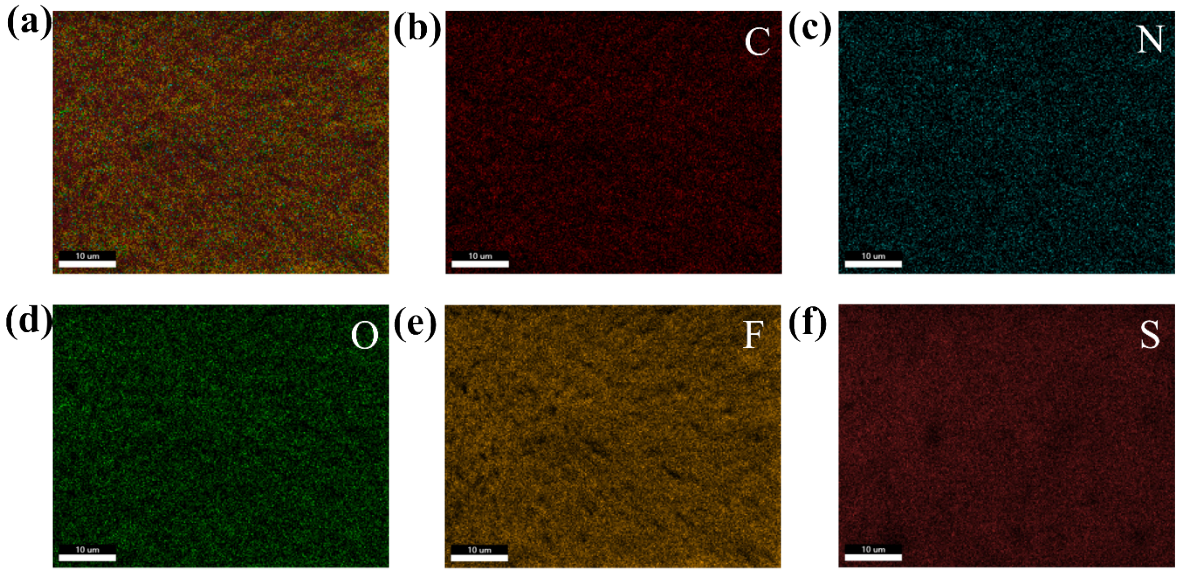


**Fig. S1** EDS mapping of PTCL−1.5 (a) mix, (b) C, (c) N, (d) O, (e) F, and (f) S elements.

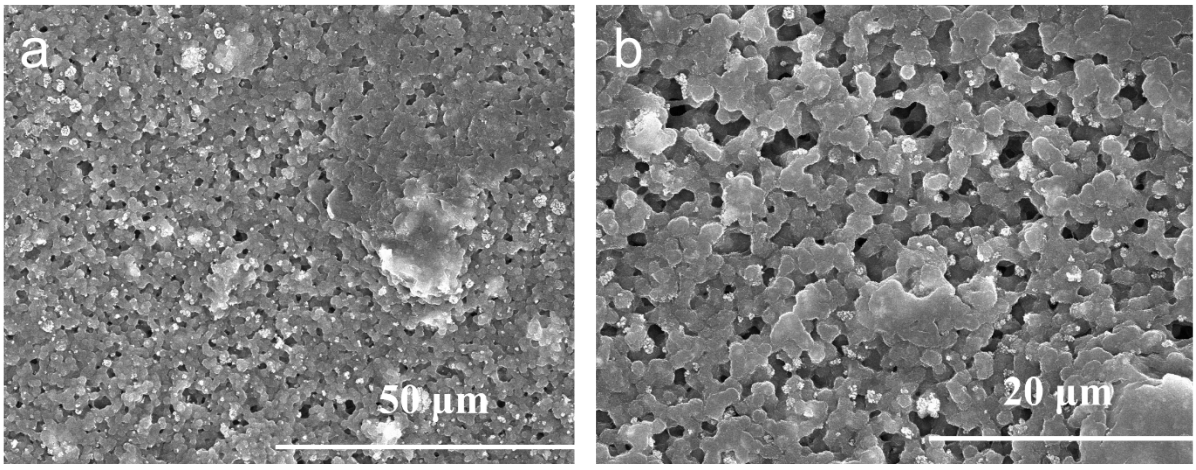


**Fig. S2** (a−b) SEM image of composite solid electrolyte film at 0.2 g lithium salts mass (PTCL−0.5).


**Fig. S3** Photograph of PTCL−1.5 thickness.

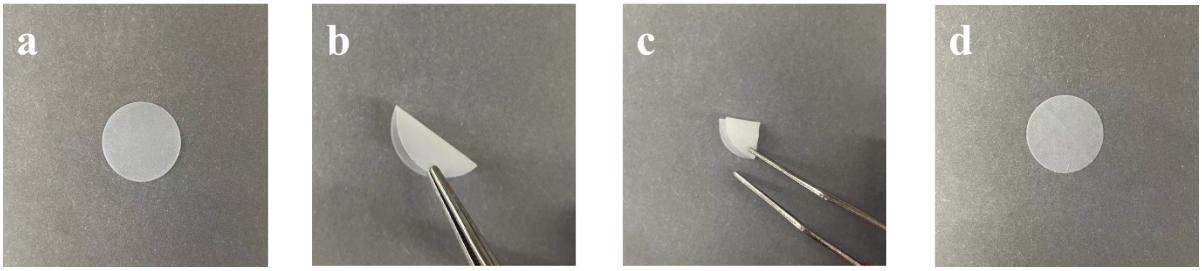


**Fig. S4** Photographs of PTCL−1.5 with different folded shapes. (a) flatten, (b) fold, (c) bi-fold, (d) flatten.

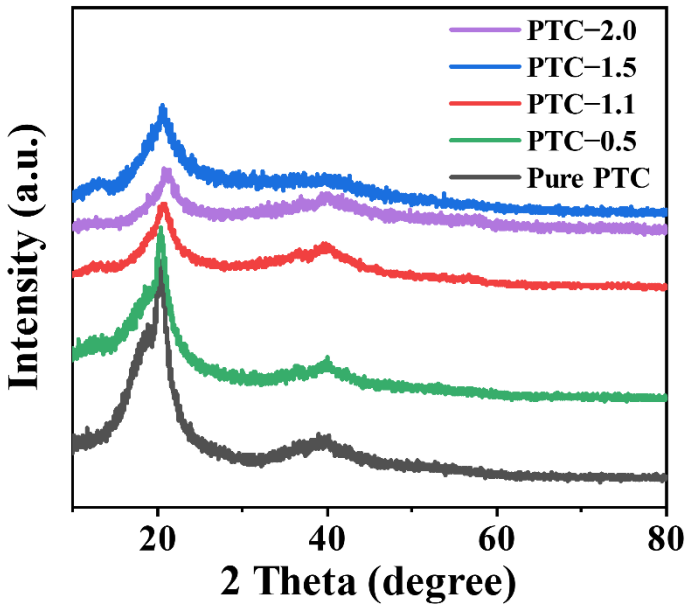


**Fig. S5** XRD patterns of different polymer membranes.

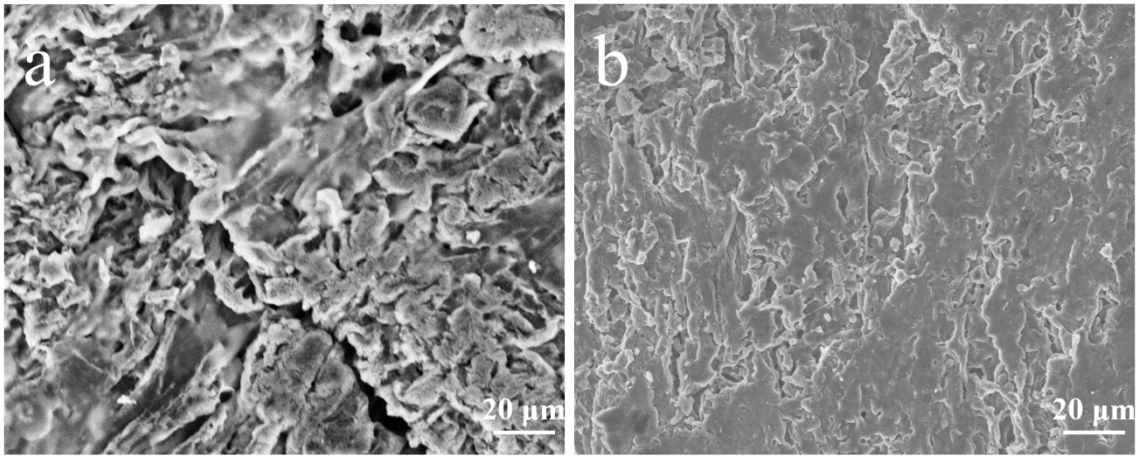


**Fig. S6** High-magnification SEM images of lithium metal anode after cycling. (a) PTC−1.5, (b) PTCL−1.5.

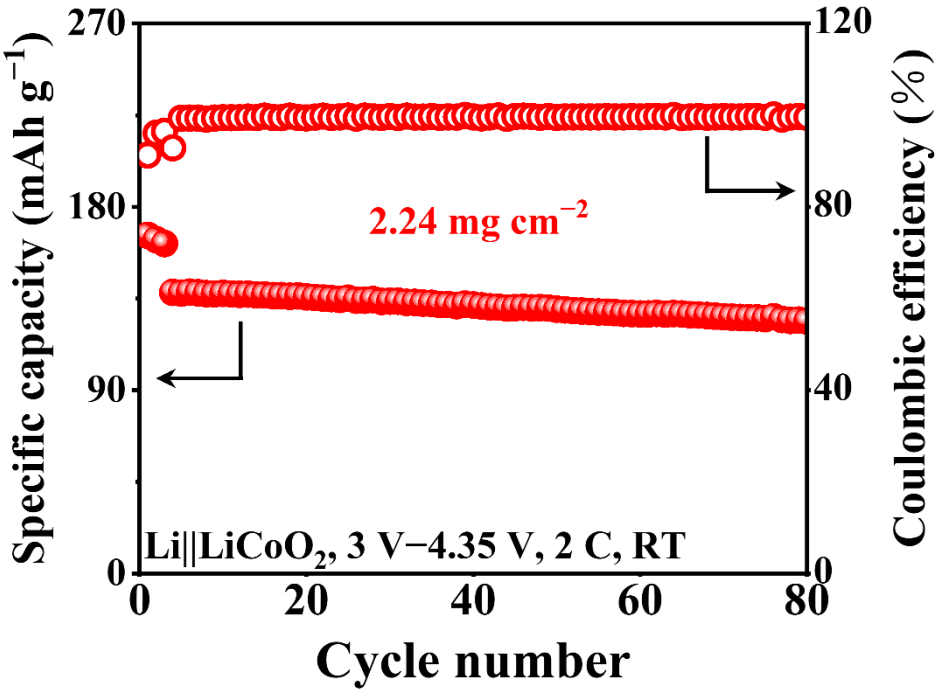


**Fig. S7** Cycling performance of Li|PTCL−1.5|$LiCoO_2$ cell at 2 C.

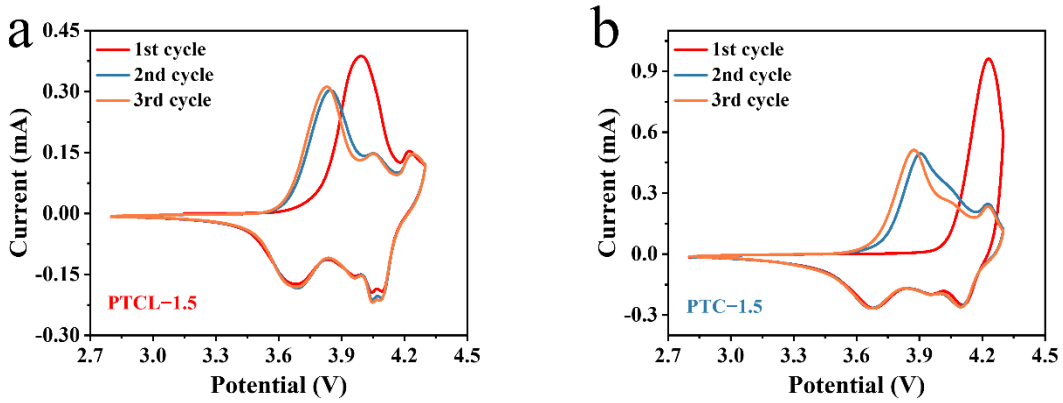


**Fig. S8** CV curves of (a) Li|PTCL−1.5 |NCM9055 and (b) Li|PTC−1.5 |NCM9055 cells. The scan rate is 0.1 mV/s.

As shown in Fig. S8a and b, in the first cycle of the CV test, the Li|PTC−1.5|NCM9055 cell exhibited greater polarisation compared to the Li|PTCL−1.5|NCM9055 cell, indicating that the Li|PTC−1.5|NCM9055 cell has poorer oxidative stability. In addition, analysis of the CV curves of the second and third cycles shows that the Li|PTCL−1.5|NCM9055 cell has a higher overlap of CV curves compared to the Li|PTC−1.5|NCM9055 cell. It indicates that PTCL−1.5 has more stable electrochemical properties compared to PTC−1.5.

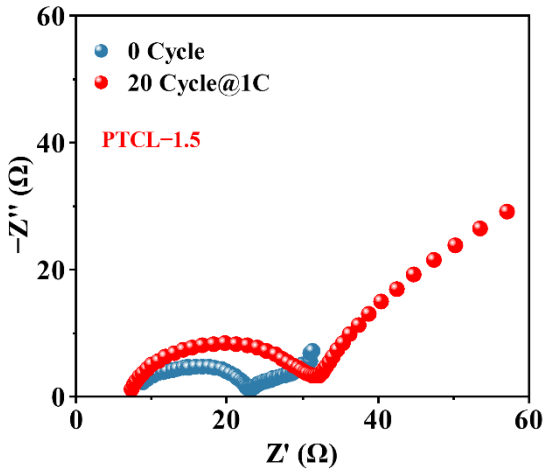


**Fig. S9** The interfacial impedance of Li|PTCL−1.5|LFP cell before cycle and after 20 cycles (1C) at RT.

To investigate the impedance changes before and after cycling, we constructed a Li|PTCL−1.5|LFP cell and performed electrochemical impedance spectroscopy (EIS) tests both before and after cycling. As shown in Fig. S9, there is only a slight increase in the interfacial impedance after 20 cycles at 1C compared to the impedance before cycling.

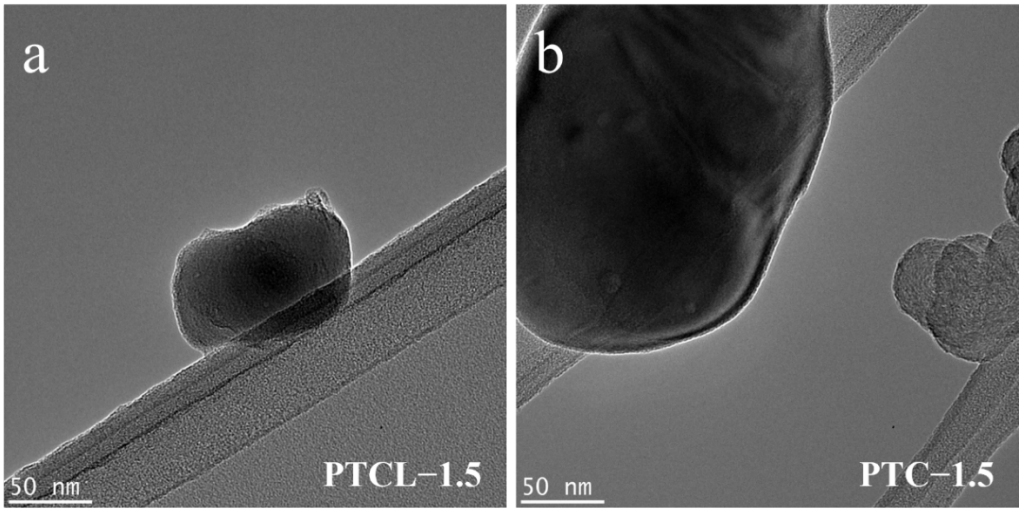


**Fig. S10** Low magnification TEM images. (a) PTCL−1.5, (b) PTC−1.5.

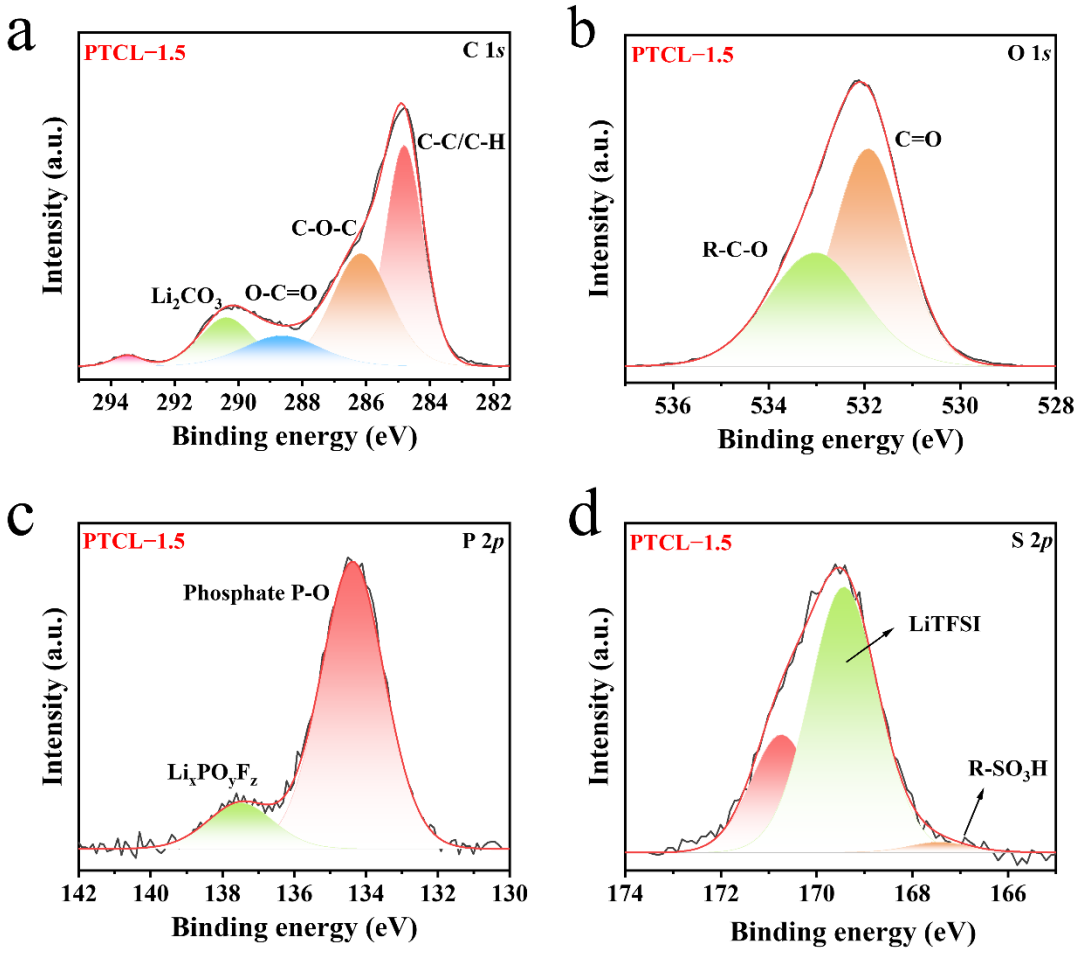


**Fig. S11** XPS spectra of PTCL−1.5 (a) C 1*s*, (b) O 1*s*, (c) P 2*p*, and (d) S 2*p*.

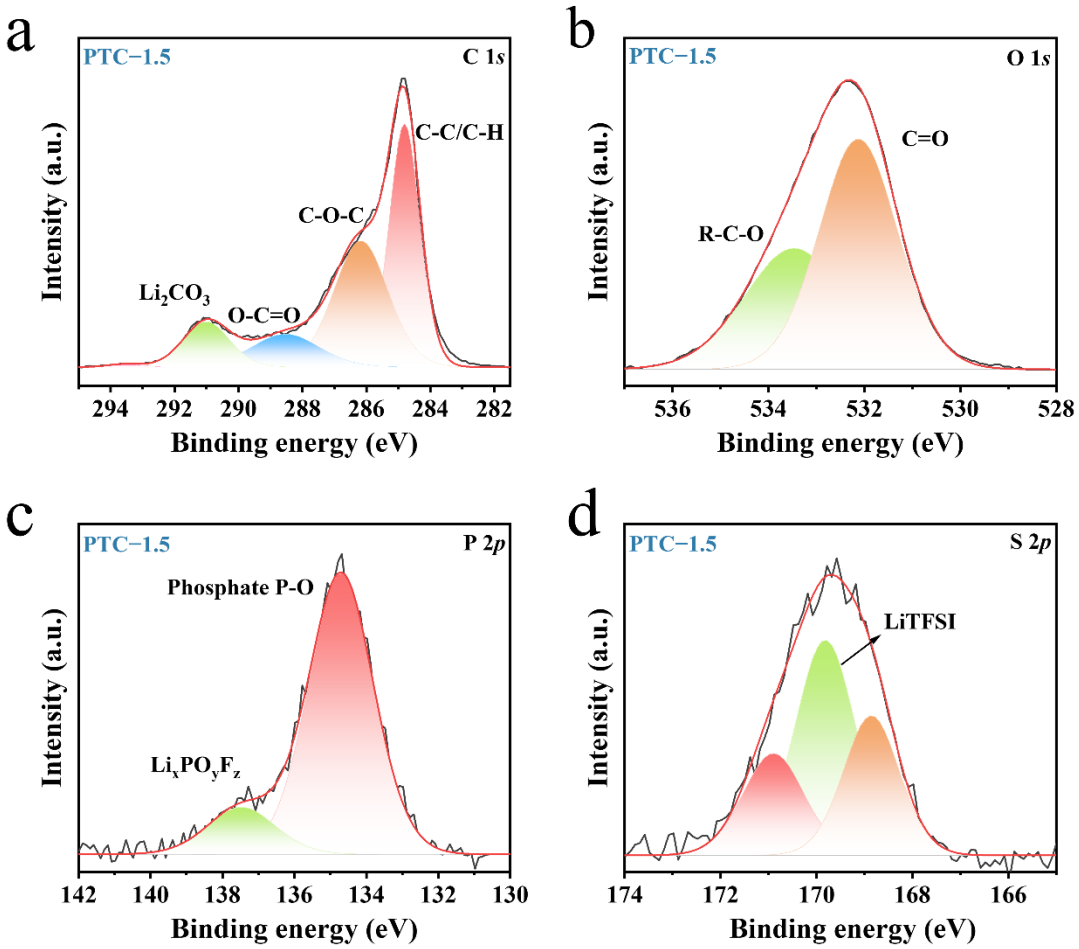


**Fig. S12** XPS spectra of PTC−1.5 (a) C 1*s*, (b) O 1*s*, (c) S 2*p*, and (d) P 2*p*.

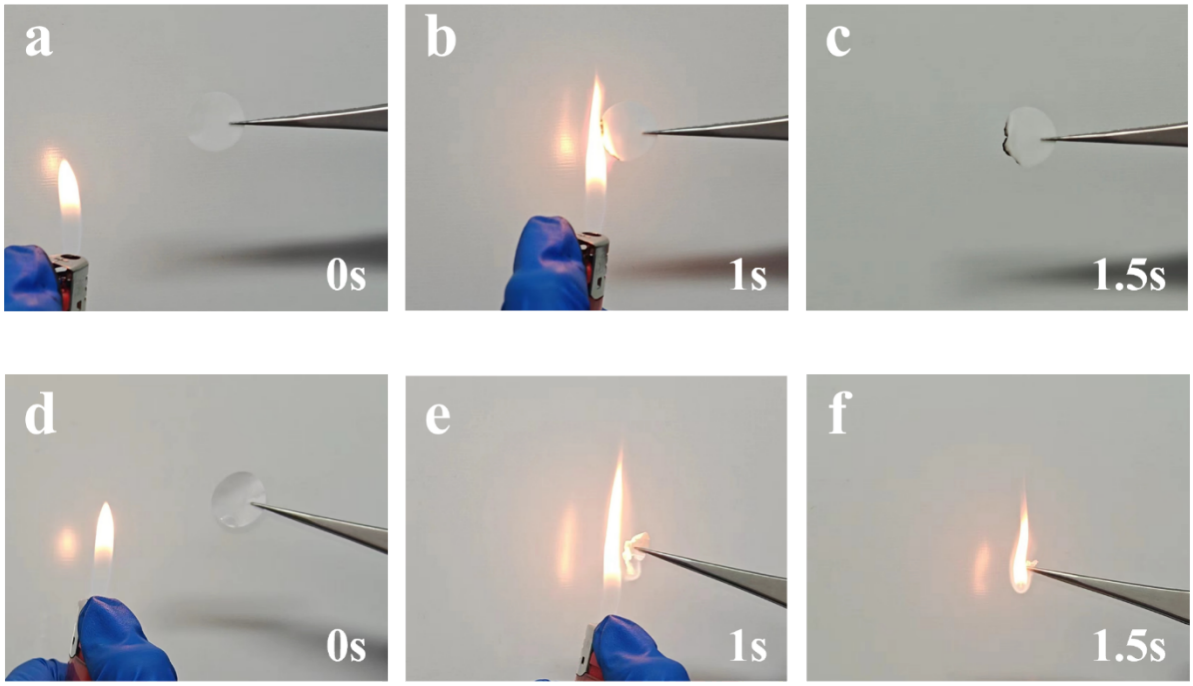


**Fig. S13** Combustion test. (a−c) PTCL−1.5, (d−f) Celgard separator immersed with LEs.


**Fig. S14** Open circuit voltage of a pouch cell.